Exocytosis of Pinocytosed Fluid in Cultured Cells: Kinetic Evidence for Rapid Turnover and Compartmentation

JEFFREY M. BESTERMAN, JUDITH A. AIRHART, ROBERT C. WOODWORTH, and ROBERT B. LOW

Department of Physiology, Milton S. Hershey Medical Center, Pennsylvania State University, Hershey, Pennsylvania 17033, and the Department of Physiology and Biophysics and Department of Biochemistry, University of Vermont College of Medicine, Burlington, Vermont 05405

ABSTRACT The uptake and fate of pinocytosed fluid were investigated in monolayers of pulmonary alveolar macrophages and fetal lung fibroblasts using the fluid-phase marker, [^{14}C]sucrose. Initial experiments revealed that cellular accumulation of chromatographically repurified [^{14}C]sucrose was not linear with incubation time. Deviation from linearity was shown to be due to constant exocytosis of accumulating marker. Chromatographic analysis revealed that the cells were unable to metabolize sucrose and were releasing it intact by a process that was temperature-sensitive but not dependent on extracellular calcium and magnesium. A detailed analysis of the kinetics of exocytosis was undertaken by preloading cells with [^{14}C]sucrose for various lengths of time and then monitoring the appearance of radioactivity into isotope-free medium. Results indicated that modeling the process of fluid-phase pinocytosis and subsequent exocytosis required at least two intracellular compartments in series, one compartment being of small size and turning over very rapidly ($t_{1/2}$ = 5 min in macrophages, 6–8 min in fibroblasts) and the other compartment being apparently larger in size and turning over very slowly ($t_{1/2}$ = 180 min in macrophages, 430–620 min in fibroblasts). Computer-simulation based on this model confirmed that the kinetics of efflux faithfully reflected the kinetics of influx and that the rate of efflux completely accounted for the deviation from linearity of accumulation kinetics. Moreover, the sizes of the compartments and magnitude of the intercompartment fluxes were such that the majority of fluid internalized in pinocytic vesicles was rapidly returned to the extracellular space via exocytosis. This result provides direct experimental evidence for a process previously thought necessary based solely on morphological and theoretical considerations. Furthermore, the turnover of pinocytosed fluid was so dynamic that accumulation deviated from linearity even within the first few minutes of incubation. We were able to show that the kinetics of exocytosis allowed calculation of the actual pinocytic rate, a rate that was nearly 50% greater than the apparent initial rate obtained from the slope of the uptake curve over the first 10 min.

Pinocytosis may represent the afferent arm of a homeostatic mechanism for recycling the plasmalemma. The foundation for this hypothesis was laid by the work of Steinman et al. (37). Their stereological analysis of pinocytosis in macrophages and L-cells revealed that the volume and surface area of incoming pinocytic vesicles was ten times greater than that which the secondary lysosomal compartment was shown to accommodate and, therefore, they postulated: (*a*) that interiorized pinocytic vesicle fluid must rapidly egress from the vacuolar system and (*b*) that pinocytic vesicle membrane is recycled back to the cell surface. Recently, the latter prediction has received experimental support both in mammalian (25, 34) and nonmammalian (6, 42) cells. These studies provided evidence for a large and rapid return flow of endocytosed membrane back to the cell surface. It was our intent to test the former prediction by closely examining the fate of pinocytosed fluid as indicated by the kinetics of the fluid-phase marker, [^{14}C]sucrose. The resolution of this question is important, not only for understanding

THE JOURNAL OF CELL BIOLOGY · VOLUME 91 DECEMBER 1981 716-727

the homeostatic mechanism by which intracellular volume is kept constant but also necessary for unequivocal quantitation of fluid-phase pinocytosis.

MATERIALS AND METHODS

Cells

Guinea pig alveolar macrophages were lavaged from lungs as previously described (23) using calcium- and magnesium-free phosphate-buffered saline (PBS). Cells were centrifuged, washed, hemocytometrically counted, and suspended in Dulbecco's PBS supplemented with one g/l glucose, pH 7.4. The cell suspension was labeled with [^{3}H]leucine (5 μCi/10 nmol per ml of suspension) for at least 1 h at 37°C. Incorporation was halted by the addition of leucine to 1 mM. The cells were then plated at ~ 3×10^6 macrophages per 35 mm Falcon tissue culture dish (Falcon Labware, Oxnard, Calif.) and allowed to form adherent monolayers for 1 h at 37°C before experiments were begun. Experimental time in culture was considered to begin at the conclusion of this 1-h adhesion period.

IMR-90 human fetal lung fibroblasts (Institute for Medical Research, Camden, N. J.) were seeded into 35-mm Falcon tissue culture dishes (Falcon Labware) at a density of 1×10^5 cells/dish and grown in Eagle's minimal essential medium (EMEM) supplemented with 10% fetal bovine serum (FBS), 2 mM L-glutamine, and chlortetracycline HCl, 100 μg/ml. Cultures were incubated at 37°C in a humidified atmosphere of room air with 5% CO_2 (Forma Incubator model 3314, Marietta, Ohio). The cultures were confluent 5–7 d after seeding and were then used without delay. A confluent 35-mm dish contained ~214 μg of protein, equivalent to 1×10^6 cells. All fibroblasts studied were in the mid-range of their in vitro lifespan (population doubling level = 20–30).

Unless specifically indicated, the medium used for experiments with macrophages was Dulbecco's PBS, pH 7.4, supplemented with one g/l glucose and a complete complement of amino acids, all at physiological levels. The medium used for experiments with fibroblasts was identical to that described above for macrophages except that it was also supplemented with 2% FBS. The pH of the media remained a constant 7.2–7.4 throughout the entire 5-h experimental period (data not shown).

Chromatographic Purification of Radiolabeled Sucrose

Chromatography of the radiolabeled sucrose (as described below) revealed that radioactive glucose and fructose were present in all commercially available preparations tested. The extent of contamination was very variable and dependent on the nature of the radiolabel, the range being 0.7–6.4% contamination for ^{14}C-labeled sucrose and 3.7–13.3% for ^{3}H-labeled sucrose. (Simultaneous but independent of this work was a report by Ose et al. [27] which indirectly came to the same conclusion.) Therefore, all radiolabeled sucrose was routinely repurified before use.

Samples were applied to strips of Whatman #1 chromatography paper (Whatman, Inc., Clifton, N. J.) by repeated spotting with a 5 μl Drummond microcap under a stream of air (Drummond Scientific Co., Broomall, Pa.). Chromatography was performed in a 28 × 60 cm cylindrical glass tank, lined with Whatman #1 paper and pre-equilibrated overnight with the *n*-butanol, ethanol (95%), water (104: 60: 20) solvent system (30) used to develop the chromatograms by descending chromatography for 14–18 h at room temperature.

For analytical purposes, the chromatographic profile was determined by slicing the chromatogram into sections 1 cm in length. Each section was folded accordion-style, placed in a scintillation vial, eluted with water for 30 min, and radioassayed with Aquasol-2 (New England Nuclear, Boston, Mass.).

For preparative purposes, a narrow strip of the chromatogram was assayed as described above to locate the sucrose peak. The sucrose peak was eluted with water from the remainder. Efficiency of recovery was 80–90%.

R_f values closely approximated published values (30) and were as follows: sucrose, 0.11; glucose, 0.17; fructose, 0.22. These values varied ± 20% depending on the mode of sample preparation. Occasionally, the two monosaccharides comigrated as one peak, but always were cleanly separated from the sucrose.

Experimental Design: Uptake and Subsequent Release of [^{14}C]sucrose

Monolayers were washed free of any nonadherent cells and incubated with medium containing [^{14}C]sucrose for various lengths of time at the indicated temperature. At the end of incubation the medium was removed with a Pasteur pipet, the monolayers rapidly washed 6 times with ice-cold PBS and the dishes quickly drained by inversion onto absorbent paper. The monolayers were immediately reincubated to study the release of radioactivity from the cells. The reincubation medium was identical to that used during incubation except that isotopically labeled sucrose was omitted. (Unlabeled sucrose was not included in this medium as preliminary experiments showed that its presence (70 μM) during reincubation did not affect results.) At intervals over the next 2 h the reincubation medium was collected and replaced with fresh medium. The cell monolayer was finally solubilized in 1% (wt/vol) SDS (except for chromatography, see below). Both media and cell fractions were assayed for radioactivity as described below.

The total radioactivity present in the cell monolayer at the commencement of reincubation was determined by adding the accumulated radioactivity released during reincubation to the radioactivity remaining associated with the monolayer.

Controls for accumulation of label at zero-time and its subsequent release were performed for each experiment to determine the efficiency of the washing procedure and the extent of [^{14}C]sucrose binding (adsorption) to, and dissociation from, the cell membrane and culture dish. From these controls it was calculated that the washing procedure left behind <0.001% of the extracellular volume and that only for incubation periods shorter than 30 min could the radioactivity contained in this volume account for >5% of the cell-associated radioactivity (e.g. for 5-min incubation periods the zero-time control represented 25% of cell-associated radioactivity in macrophages and 35% in fibroblasts). For all kinetic studies reported, release after a zero-time loading was subtracted from reported values.

For chromatography, the cell monolayer was solubilized in 1 M NH_4OH, evaporated to dryness under a stream of nitrogen gas, redissolved in water and, after addition of three volumes of 95% ethanol, chilled overnight. The ensuing precipitate was then pelleted by low speed centrifugation and the supernate evaporated to a final volume of ~50 μl and chromatographed as described.

Radioassay

Radioassay for ^{3}H and ^{14}C was performed with the scintillant, Aquasol-2 (New England Nuclear), on a Packard Tri-Carb liquid scintillation spectrometer, Model 3320, (Packard Instrument Co., Inc., Downers Grove, Ill.) with an average efficiency of 28% for ^{3}H, 37% for ^{14}C, and 25% spill of ^{14}C into the ^{3}H channel. Quench and spill were monitored by external standard.

Protein Determination

Protein content of solubilized cell monolayers was determined by the method of Lowry (24) using bovine serum albumin as a standard.

Materials

The following materials were obtained from the indicated sources: male guinea pigs. Canadian Breeders Laboratories, St. Constant, Quebec, Canada; Dulbecco's PBS, Gibco Laboratories, Grand Island Biological Company, Grand Island, N. Y.; 35 mm tissue culture dishes, Falcon Labware, Oxnard, Calif.; Whatman #1 chromatographic paper, VWR Scientific Inc., San Francisco, Calif. (manufactured by Whatman, Inc., Clifton, N. J.); fetal bovine serum and Eagle's minimal essential medium, Microbiological Associates, Walkersville, Md.; bovine serum albumin and yeast invertase, grade X from *Candida utilis*, Sigma Chemical Co., St. Louis, Mo.; [6,6′(n)-^{3}H]-sucrose 5Ci/mmol, [^{14}C(U)]-sucrose 477 mCi/mmol, and L-[4, 5-^{3}H]-leucine 50 Ci/mmol, Amersham Corp., Arlington Heights, Ill.; [^{14}C(U)]-sucrose 673 mCi/mmol, [6,6′(n)-^{3}H]-sucrose 5Ci/mmol, and Aquasol-2, New England Nuclear, Boston, Mass. All other chemicals were reagent grade.

RESULTS

Kinetics of [^{14}C]sucrose Accumulation

Monolayers of pulmonary alveolar macrophages and IMR-90 fetal lung fibroblasts accumulated [^{14}C]sucrose at a rate that decreased with time (Fig. 1). This was the finding one would expect if the cells were in net volume balance, that is, once the exocytic rate of the accumulating marker started to approach the endocytic rate of marker in the medium, the intracellular compartment(s) began to approach steady state. However, there were at least two alternate explanations that had to be investigated: (*a*) The cell's pinocytic activity was decreasing as a function of time in culture. (*b*) The [^{14}C]sucrose was being internalized, degraded, and the radiolabeled degradation products were escaping from the cell.

To test the first alternative, sets of monolayers were coincubated in the presence of tracer levels of unlabeled sucrose. At

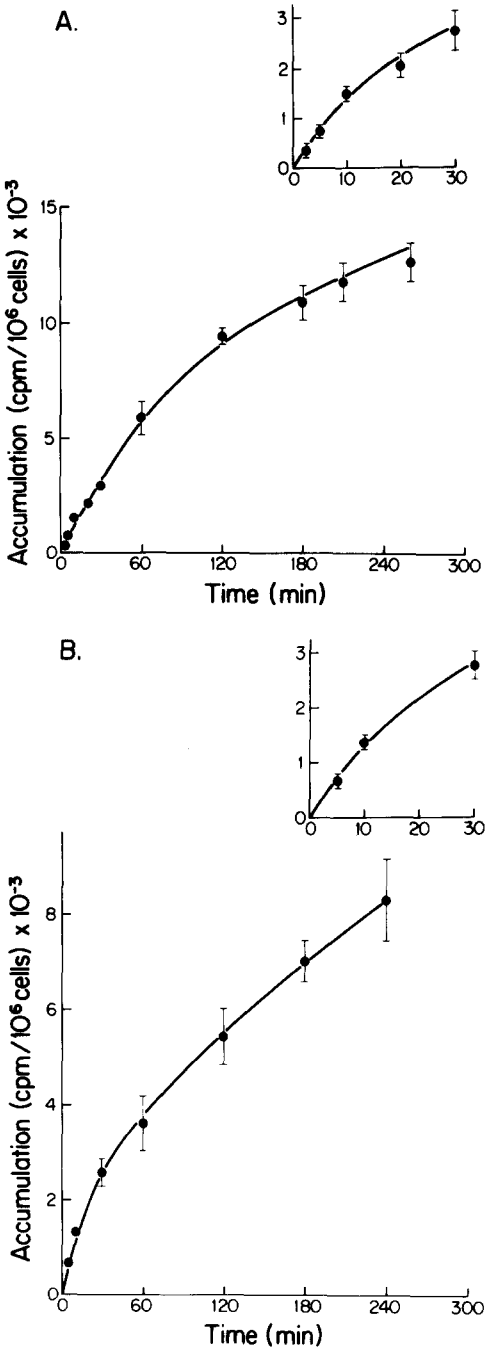

FIGURE 1 Kinetics of accumulation of [^{14}C]sucrose by cultured pulmonary alveolar macrophages and IMR-90 fibroblasts. Cell monolayer of 3 × 10^6 macrophages (A) or confluent monolayers of 1 × 10^6 fibroblasts (B) were incubated for specified periods at 37°C with medium containing [^{14}C]sucrose. Insets provide magnified view of accumulation over the first 30 min of incubation. For cells incubated at 4°C, accumulation in 2 h ranged from 2–15% of that occurring at 37°C (data not shown). Details of cell culture, washing procedure, and determination of cell accumulated radioactivity are described in Materials and Methods. Accumulation was calculated by summing the total radioactivity released during reincubation with the radioactivity remaining associated with the monolayer or as the total radioactivity present in the monolayer before reincubation. Identical results were obtained with both protocols. Therefore, results were combined and each data point represents the mean ± SD of 2–4 experiments, each experiment performed in duplicate. All values were normalized to the [^{14}C]sucrose concentration used for the shortest incubation periods (27 cpm/nl for macrophages; 39 cpm/nl for fibroblasts). Curves were drawn by eye.

the beginning of each hour over the next 3 h, [^{14}C]sucrose was added to one set of cultures and cell-associated radioactivity measured 1 h thereafter. Table I shows that the rate of [^{14}C]sucrose accumulation over succeeding 1-h periods remained constant. Furthermore, we incubated one set of monolayers with [^{14}C]sucrose for 1 h, then transferred this medium to a second set of monolayers that had already been in culture for 3 h and assayed for cell-accumulated radioactivity 1 h later. Results were identical in pre- and posttransfer cultures (Table I). Therefore, we concluded that the cells remained fully active throughout the experiment and that the progressive decrease in the rate of [^{14}C]sucrose accumulation could not be due to inherent deterioration of the cells or an adverse effect brought on by some cell-associated, time-dependent change in the medium. In line with this conclusion, the possibility that decreasing accumulation with time could be due to depletion of isotopic sucrose from the medium was easily ruled out because only 0.3% of the [^{14}C]sucrose in the medium was cell-associated after 4 h of incubation.

To determine whether the cultured cells were metabolizing [^{14}C]sucrose and releasing the degradation products or simply releasing intact [^{14}C]sucrose, we pulsed monolayers for 1 h with [^{14}C]sucrose, chased with [^{14}C]sucrose-free medium for 1 h, and analyzed the chase medium and solubilized cell monolayers by paper chromatography and radioassay. Chromatographic analysis revealed that >98% of the released radioactivity was [^{14}C]sucrose. Likewise, it was found that >98% of the radioactivity remaining associated with the cell layer was [^{14}C]sucrose. Commensurate with this, no radiolabeled degradation products of sucrose were detectable in either the chase medium or the cell layer (data not shown). Finally, the total radioactivity associated with the cells at the commencement of the chase was recoverable from the chase medium and cell layer, indicating no significant loss of label due to metabolism of [^{14}C]sucrose to $^{14}CO_2$. Thus, this experiment provided direct evidence that alveolar macrophages and lung fibroblasts released previously accumulated [^{14}C]sucrose, released it intact, and did not metabolize sucrose in culture.

Origin and Significance of [^{14}C]sucrose Release

A number of experiments were performed to determine the nature of the release process. In the following sections only the

TABLE I

Effect of Incubation Time on Cellular Accumulation of [^{14}C]sucrose

Length of incubation before pulse (h)	[^{14}C]sucrose accumulation during 1 h pulse	
	cpm/ 10^6 cells	
	macrophages	*fibroblasts*
0	6072 ± 184	3952 ± 88
1	6376 ± 64	—
2	6560 ± 264	3896 ± 168
3*	5707 ± 285	4272 ± 280

Monlayers of either 3 × 10^6 pulmonary alveolar macrophages or 1 × 10^6 IMR-90 fibroblasts were incubated in the presence of 1 μM unlabeled sucrose. At the beginning of each hour, [^{14}C]sucrose was added to the medium of one set of monolayers and cell-associated radioactivity assayed 1 h thereafter. The zero-time control value has been subtracted from all determinations. Each value is the mean of triplicate determinations and is expressed ± SD.

* Instead of receiving fresh radiolabeled medium, these monolayers received the radioactive medium used during the first 1-h interval for a different set of monolayers.

macrophage data will be presented in detail. Results obtained in an identical manner on fibroblasts will be provided in a summarized form for comparative purposes.

Macrophages were incubated in medium containing [^{14}C]-sucrose for 1 h after which the medium was removed, the monolayers rapidly and thoroughly washed, drained, and reincubated with isotope-free medium under specified conditions. Table II shows that release was sensitive to temperature and did not require extracellular calcium and magnesium (at least at a concentration >1 nM). These two results argue in favor of the hypothesis that release is a manifestation of continuous exocytosis. To support this hypothesis further, we sought to eliminate the possibility that released [^{14}C]sucrose was merely derived from binding to, and temperature-dependent dissociation from, the plasma membrane or culture dish. Table II shows that in the presence of invertase at 4°C, no additional radioactivity was released above that which was normally released at 4°C. This same result was also obtained in medium containing invertase plus excess glucose and fructose, the latter two components added to insure against uptake of [^{14}C]glucose and [^{14}C]fructose in the event that [^{14}C]sucrose was accessible to the hydrolytic action of invertase at 4°C (Table II). Incubation of [^{14}C]sucrose and invertase together under conditions identical to those used in Table II (line 4) revealed that 35% of the [^{14}C]sucrose was hydrolyzed to [^{14}C]glucose and [^{14}C]fructose in 1 h (data not shown), confirming the activity of the enzyme under these adverse incubation conditions (nanomolar levels of sucrose, 4°C, pH 7.2). Thus, were the releasable [^{14}C]sucrose initially trapped extracellularly or bound to the cell membrane, we would have expected to see a doubling in released radioactivity in the presence of invertase. This was not the case (Table II). Furthermore, cells exposed to [^{14}C]sucrose for 1 h at 4°C, washed and reincubated for 20 min at 37°C, released only 10–15% of the radioactivity released after a 1-h loading at 37°C (data not shown). Finally, we recently have found that the release process is modulated by physiological levels of amino acids (Besterman, Airhart, and Low, manuscript submitted for publication) an unlikely occurrence if simple dissociation of adsorbed sucrose was involved. Taken together, these findings provide further evidence that release is the expression of exocytosis and not merely an artifact of experimental protocol.

TABLE II

Characterization of [^{14}C]sucrose Release by Alveolar Macrophages

Modification of standard reincubation conditions	CPM released/10^6 Cells	
	0–10 Min	10–60 Min
None	869 ± 52	897 ± 43
$-Ca^{++}/Mg^{++}$	781 ± 70	866 ± 103
4°	246 ± 41	171 ± 24
4° + invertase, −glucose	260 ± 51	135 ± 20
4° + invertase, +glucose, +fructose	238 ± 60	145 ± 38

Monolayers of 3 × 10^6 pulmonary alveolar macrophages were incubated in medium containing [^{14}C]sucrose for 1 h at 37°. The medium was then rapidly and thoroughly removed as described in the text and the monolayers immediately reincubated in isotope-free media under the conditions specified in the table. Standard reincubation conditions were: Dulbecco's PBS supplemented with 1 mg/ml glucose and a complete complement of amino acids, pH 7.4, 37°. When present, fructose was at a final concentration of 1 mg/ml and invertase at 100 U/ml. The minus Ca^{++}/Mg^{++} condition was obtained by addition of EDTA to 1 mM, which reduced the free concentration of these two ions to below nanomolar levels as calculated using available affinity constants (36). Data are expressed as the mean ± SD, n=3.

Next, we wished to test the possibility that [^{14}C]sucrose release merely reflected cell death or detachment during the course of incubation. Before exposure to [^{14}C]sucrose, macrophages were pulsed with [^{3}H]leucine for 1 h to isotopically label cellular protein (see Materials and Methods; also see references 4, 22, and 28). By doing so, the exocytosed [^{14}C]-sucrose could be corrected for the contribution from sloughed-off cells that contained [^{14}C]sucrose. Based on the ^{14}C:^{3}H ratio in the intact monolayer, at most, 11% of the [^{14}C]sucrose released in 1 h could have been due to this alternate source (data not shown). This figure is certainly an overestimation because some portion of the released ^{3}H is not due to cell loss from the monolayer but simply due to normal turnover and secretion of protein.

Finally, Fig. 2 demonstrated that both [^{14}C]sucrose accumulation and its subsequent release were directly proportional to cell number and [^{14}C]sucrose concentration – supporting the premise that [^{14}C]sucrose enters the cell by fluid-phase pinocytosis and remains a component of the fluid-phase while on its journey through the cell and back into the extracellular milieu.

Kinetics of Exocytosis

To describe the process of sucrose release more completely, macrophage monolayers were incubated with [^{14}C]sucrose for various lengths of time (loading time) and the kinetics of exocytosis monitored by subsequent reincubation in isotope-free medium (Table III). Three observations were immediately apparent from these data: (*a*) the rate of [^{14}C]sucrose exocytosis decreased with increasing length of reincubation, regardless of loading time; (*b*) the absolute amount of [^{14}C]sucrose exocytosed in 120 min increased with increasing loading time and appeared to approach a maximum value; and (*c*) of the total [^{14}C]sucrose present in the cell monolayer at the commencement of reincubation, the percentage exocytosed in 120 min decreased with increasing loading time and appeared to approach a minimum value.

Fig. 3 *A* expresses these data as the percentage of [^{14}C]sucrose remaining inside the cells as a function of reincubation time. It was apparent that the kinetics of exocytosis could not be described by a single exponential process; rather, a minimum of two exponentials were required to fit these data. Virtually identical kinetic parameters were obtained regardless of the length of loading, that is, there was first a rapid loss ($t_{1/2}$ = 5 min, see below) followed by a much slower release ($t_{1/2}$ = 180 min). The half-life of the faster component was obtained by extrapolation of the slower component back to the ordinate and the values so generated subtracted, point-for-point, from the faster component ("curve peeling"; [17]). The difference curve is plotted in Fig. 3 *B*, the slope being a function of the half-life of the faster component only.

The *y* intercepts obtained by back extrapolation of the slower component were taken as a measure of the distribution of the [^{14}C]sucrose among two kinetically defined intracellular compartments. Thus, after a preload of 5 min, ~35% of the intracellular [^{14}C]sucrose behaved kinetically as if it was located in the slowly turning over compartment whereas after a preload of 120 min or greater, ~90% of the [^{14}C]sucrose is found in the slower compartment.

The true endocytic rate can be calculated from these data describing the kinetics of exocytosis with the only assumption being that the cell's volume remains constant. This was accomplished by determining the size and turnover rate of each

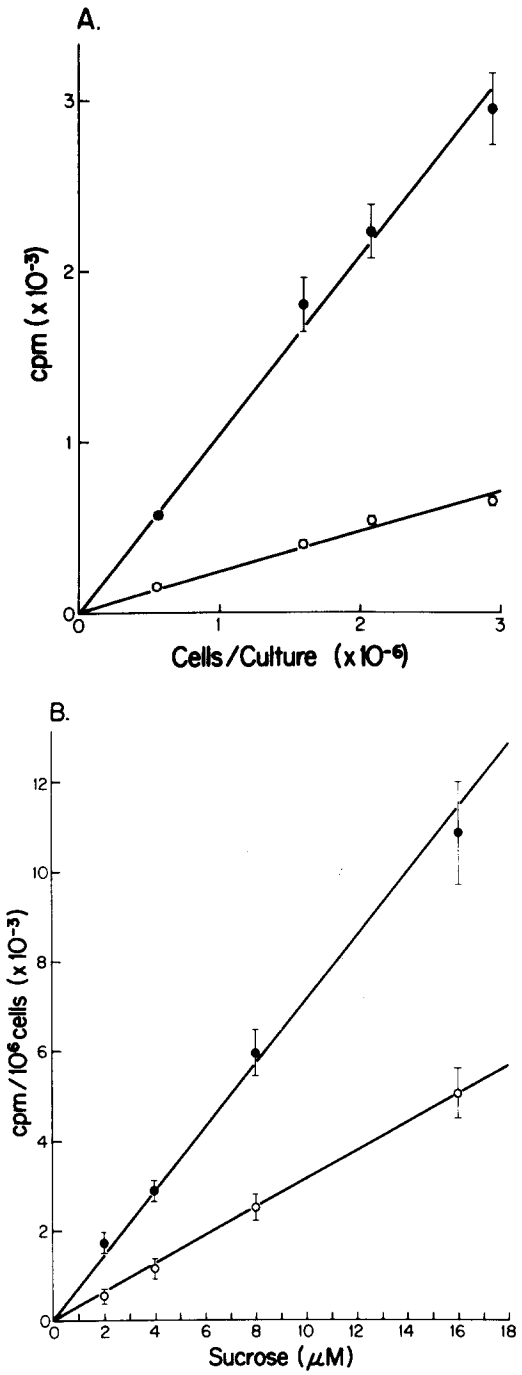

FIGURE 2 Accumulation (●) and release (○) of [^{14}C]sucrose by macrophage monolayers as a function of [^{14}C]sucrose concentration and cell density. (*A*) Macrophage monolayers of various cell numbers were incubated at 37°C with 6 μM [^{14}C]sucrose for 2 h (accumulation), washed free of radiolabeled sucrose, and reincubated in tracer-free medium at 37°C for 1 h (release). (*B*) Monolayers of 3 × 10^6 macrophages were incubated with varying concentrations of [^{14}C]sucrose at 37°C for 4 h (accumulation) washed free of radiolabeled sucrose, and reincubated in tracer-free medium at 37°C for 2 h (release). Each data point is given as the mean ± SD for 2–4 determinations.

compartment. By example, for macrophages, after 180 min of incubation, 10% of the cell accumulated radioactivity turns over rapidly ($t_{1/2}$ = 5 min) while 90% turns over very slowly ($t_{1/2}$ = 180 min; Fig. 3*A*). Therefore, of the 11,100 cpm accumulated intracellularly in 180 min of incubation (Fig. 1*A*) 1,110 cpm were located in the fast compartment and 9,990 cpm were located in the slow compartment. Because the fast compartment was already at steady state, it's "size" was 1,110 cpm whereas the size of the slow compartment, because it was only "half-full", was twice 9,990 or 19,980 cpm (Table IV). From the $t_{1/2}$ of the two compartments, the fractional turnover rates (called k, having units of %/min) for each compartment could be obtained from the equation: $k = 0.693/t_{1/2}$ (35). This fractional turnover rate multiplied by the size of the compartment yields the absolute turnover rate (called K, having units of cpm/min). Thus, at steady state, 154 cpm were exocytosed from the fast compartment each min while 80 cpm were exocytosed from the slow compartment each min. Therefore, each min 234 cpm were exocytosed from the cell as a whole and consequently 234 cpm must have been endocytosed per min at steady state. Thus, the true exocytic rate was 234 cpm/min (Table IV).

Having concluded that at least two exponential processes were required to describe the observed kinetics, we next asked whether these two processes (compartments) were acting in parallel or in series. Because in a sequential model the slow compartment must be the second one to fill (designated compartment 2), an analysis of the kinetics of filling of this compartment would allow us to distinguish between the two models. By knowing the kinetics of total intracellular accumulation of [^{14}C]sucrose (Fig. 1) and the size and half-life of the fast compartment (Table IV), we were able to determine at each time-point how much of the total intracellular [^{14}C]sucrose was in the fast compartment, and, thus, by subtraction, how much was in the slow compartment. Fig. 4*A* presents the initial kinetics of accumulation of [^{14}C]sucrose into the slow compartment, determined as just described. It is apparent that there is a lag in the initial appearance of isotope into this compartment. This fact alone is evidence that the slow compartment does not fill directly from the isotopic source, namely, the extracellular medium. Moreover, if the accumulation of [^{14}C]-sucrose into the slow compartment is now replotted as a function of t^n (where n is any integer ≥1; Fig. 4*B*), that value of n which linearizes the data is a measure of how many intermediate compartments lie between the compartment of interest (slow) and the source (see Appendix I for derivation of this analysis). If linearization occurs when n = 1, then there are no intermediate compartments and the compartment of interest fills directly from the source. If n must equal 2, as it does in Fig. 4*B*, then this indicates that isotope passes through one intermediate compartment before reaching the compartment of interest, which in this case is the slow compartment. It can also be seen in Fig. 4*B* that when n is overestimated (e.g. n = 3), a nonlinear relationship is once again obtained.

Additional verification of the sequential model was obtained as follows: the slope of Fig. 4*B* with n=2 (450 cpm/59 min^2) is equal to $(K_1)(k_2)/2$ (see derivation), where K_1 is the absolute rate constant for flux from the medium to compartment 1 and k_2 is the fractional rate constant for flux from compartment 1 to compartment 2, as diagramed in Fig. 5. Because the value of K_1 had been determined to be 234 cpm/min (see above), k_2 remains the only unknown and from this equation was calculated to be 6.5%/min. Another independent approach also allowed determination of k_2: K_2 equals k_2 times the size of compartment #1. Rearranging and substituting in the previously determined values for K_2 and the size of compartment #1 (see above): $k_2 = K_2$/size of compartment #1 = 80 cpm/min divided by 1,110 cpm = 7.2%/min. The fact that nearly

TABLE III

Kinetics of [^{14}C]sucrose Intracellular Accumulation and Subsequent Exocytosis

Reincubation time	^{14}C-sucrose release after various loading times (min)						
min	*cpm/10^6 cells*						
	0	*5*	*10*	*30*	*60*	*120*	*180*
0–10	111	476	779	811	945	1107	1249
10–20	3	61	91	204	281	377	513
20–40	0	50	75	203	384	608	720
40–60	0	21	44	139	304	672	608
60–80	0	12	47	115	240	532	528
80–100	0	—	—	111	192	408	368
100–120	0	—	—	110	216	440	368
Total cpm released in 120 min	114	620	1036	1593	2608	4064	4352
CPM remaining in cells	20	190	440	1318	2884	6180	7660
Total cell-associated cpm before reincubation	134	810	1476	2911	5492	10244	12012
Percent of total cell-associated cpm released in 120 min		75	69	53	47	39	36

Monolayers of 3 × 10^6 pulmonary alveolar macrophages were incubated in medium containing [^{14}C]sucrose at 37° for various lengths of time (loading time). The medium was then rapidly and thoroughly removed as described in text and the monolayers immediately reincubated in isotope-free medium at 37° to study the release of radioactivity from the cells. At specified intervals over the next 120 min, the medium was collected and replaced with fresh medium. The cell monolayer was solubilized at the conclusion of the 120 min reincubation. All fractions were assayed for radioactivity (expressed in cpm) as described in Materials and Methods.

identical values of k_2 were obtained in both cases provides another strong argument in favor of accepting the conclusion that the sequential model is correct.

Model Testing by Computer Simulation

Until now we have tacitly assumed that the kinetics of exocytosis were the same as for endocytosis. We tested this assumption by determining whether the kinetic constants derived solely from monitoring exocytosis were capable of accurately describing endocytosis when used in a computer program designed to simulate the sequential model (Appendix IIA). Fig. 6 shows the remarkably close fit between the computer-simulation and experimental time-courses of intracellular accumulation. Thus, we conclude (*a*) that the kinetics of [^{14}C]sucrose efflux faithfully reflect the kinetics of [^{14}C]sucrose influx and (*b*) that the rate of efflux alone completely accounts for the deviation from linearity of accumulation kinetics.

DISCUSSION

Steinman et al. (37) have shown from their stereological studies that the process of pinocytosis must involve the very rapid exchange of fluid volume into and out of the cell. A major goal of our studies was to monitor the movement of a fluid-phase marker through the cell, thus directly quantitating the dynamics of the system. To follow the movement of pinocytosed liquid we chose to use the fluid-phase marker, [^{14}C]sucrose, for the following reasons. It has been shown that the cell membrane is impermeable to sucrose (7), that sucrose is not metabolized by peritoneal macrophages (9), liver (20), or other cell types (16), that sucrose does not adsorb to the cell membrane (44), and that sucrose at tracer levels does not affect the rate of fluid-phase pinocytosis as indicated by other fluid-phase markers (32).

The results described in this work demonstrated that (*a*) the rate of accumulation of [^{14}C]sucrose by monolayers of pulmonary alveolar macrophages or fetal lung fibroblasts decreases with time (Fig. 1); (*b*) that this decrease is due to release of previously accumulated [^{14}C]sucrose intact; (*c*) that at least two intracellular compartments are required to describe the kinetics of exocytosis (Fig. 3); (*d*) that these two intracellular compartments are arranged sequentially rather than in parallel (Fig. 5); (*e*) that these two compartments appear to have distinctly different half-lives and sizes, one compartment being small and turning over very rapidly and the other being apparently larger and turning over very slowly (Table IV); (*f*) that using the kinetic constants derived from monitoring exocytosis, computer generated accumulation curves very closely matched observed accumulation kinetics (Fig. 6), confirming our conclusion that, had exocytosis not occurred, accumulation would have been strictly linear with incubation time; and (*g*) that the kinetic constants describing exocytosis can be used to calculate accurately rate constants describing endocytosis.

Our results have culminated in the working model summarized in Fig. 5. A salient feature of the model is that it accomodates the observation that accumulation of a fluid-phase marker deviates from linearity very early in its time-course. It should be noted, however, that the literature is replete with apparent contradiction concerning this matter; some investigators have reported linearity up to 6 h (1, 2, 29, 32), others have provided results in agreement with our own (27, 38), while still others have reported linear accumulation of one fluid-phase marker and nonlinear accumulation of another in the same cell type (12, 31). In some cases there may be a methodological explanation for why "linear" accumulation was obtained. For example, Davies and Ross (12) found that accumulation of [^{14}C]sucrose by Swiss 3T3 cells appeared linear for up to 6 h while we have observed nearly linear [^{14}C]sucrose accumulation for 3 h in rabbit alveolar macrophages (4). The protocol used by Davies and Ross required a prolonged washing regimen (reincubation for 30 min at 37°) after the loading period, as did our past protocol (for unrelated reasons). However, we have now found that the radioactivity remaining associated with a cell monolayer after a chase period behaves far more linearly with time than does the actual accumulated radioactivity (Table III, *CPM remaining in cells*). This quirk may explain why accumulation appeared to be linear in both cases.

A cornerstone of our model is the dynamic role of exocytosis in cellular volume homeostasis, as illustrated by release kinetics. A search of the literature found references to release of intracellularly accumulated pinocytic markers in a host of in

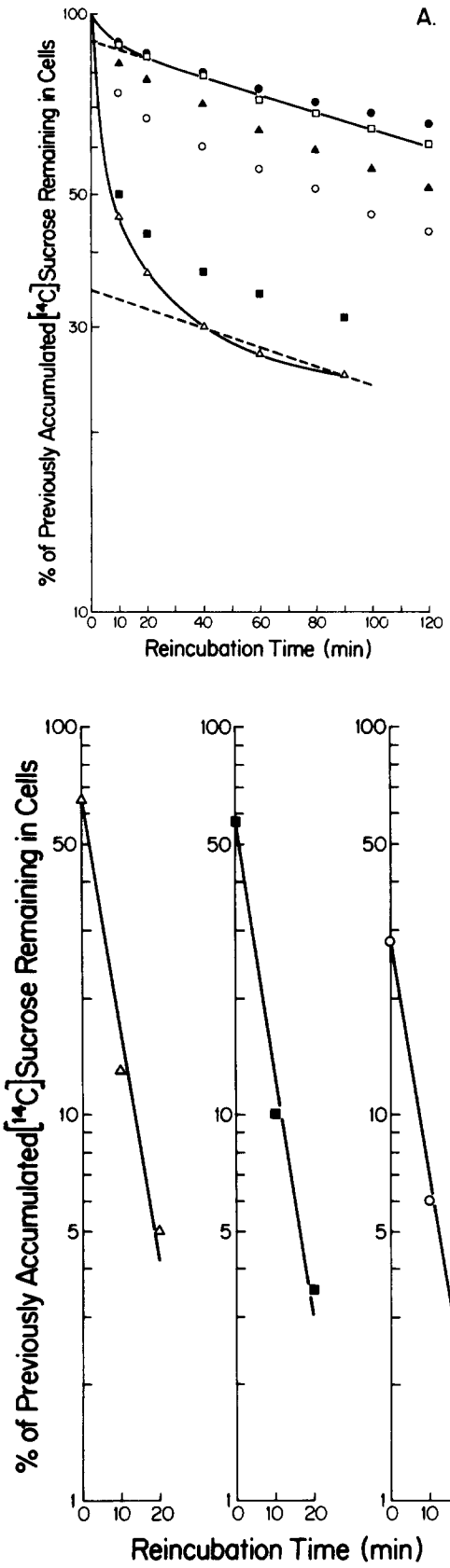

FIGURE 3 Kinetics of exocytosis of [^{14}C]sucrose by monolayers of pulmonary alveolar macrophages. (*A*) Cells were preloaded at 37° with [^{14}C]sucrose for 5 (Δ), 10 (■), 30 (○), 60 (▲), 120 (□), or 180 (●) min. The monolayers were then washed and reincubated in isotope-free medium for 120 min at 37°C, as described in Materials and Methods. Each data point represents the mean of duplicate determinations from a single representative experiment. Six such experiments were performed. For the sake of clarity, curves are drawn for the 5 and 120 min data only. Solid lines (—) represent curves drawn by eye describing all data points. Dashed lines (- - -) represent straight line approximation of lattermost time points ($t_{1/2}$ = 180 min). Data analysis ("curve peeling") was performed as described in text. The resultant difference curves are plotted in (*B*) for 5 (Δ), 10 (■), and 30 (○) min preloads.

TABLE IV

Characteristics of Intracellular Compartments and Associated Fluxes Involved in Fluid-Phase Pinocytosis

	Macrophages		Fibroblasts	
	Compartment 1	Compartment 2	Compartment 1	Compartment 2
Half-life (min)	5	180	6–8	430–620
Size (cpm/10^6 cells)	1,110	19,980	1,650	30,000
k_{efflux} to medium (%/min)	13.9	0.4	8.7–11.5	0.11–0.16
k_{efflux} to medium (cpm/min·10^6 cells)	154	80	144–190	35–51
Total k_{efflux} = total K_{influx} (cpm/min·10^6 cells)	234		179–241	

Values were determined as described in text using data from Figs. 1 *A* and 3 for macrophages and Fig. 1 *B* and data analogous to that in Fig. 3 for fibroblasts.

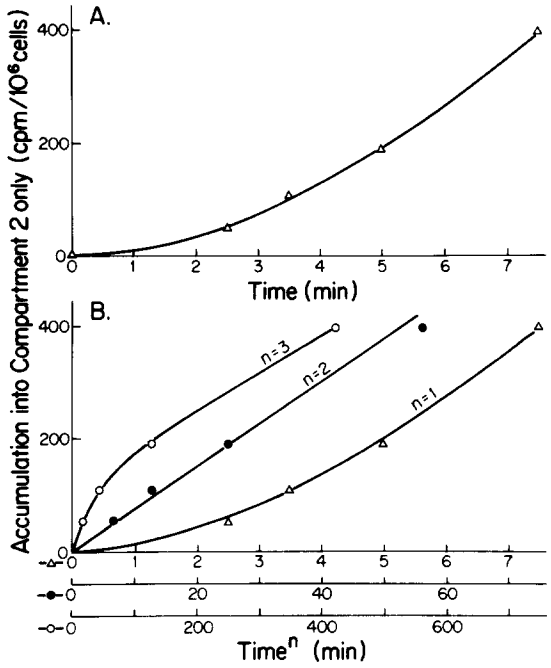

FIGURE 4 (*A*) Initial kinetics of accumulation of [^{14}C]sucrose into the slow compartment (compartment 2) of macrophages. Each data point represents a calculated value, as described in text. (*B*) Accumulation of [^{14}C]sucrose into the slow compartment (compartment 2) of macrophages as a function of time raised to the power *n* (where *n* is any integer ≥ to 1). Data (calculated as described in text) are plotted as a function of $n=1$ (Δ), $n=2$ (●), and $n=3$ (○). Curve for $n=1$ is identical to that of (*A*). Note the different time scales used.

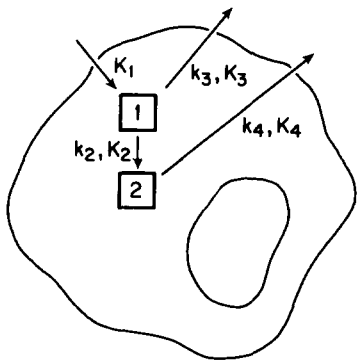

FIGURE 5 Sequential model depicting the kinetically defined compartments and fluxes involved in fluid-phase pinocytosis and exocytosis in alveolar macrophages and fibroblasts. *K*'s are absolute rate constants and *k*'s fractional rate constants. Values for these parameters are given in text and Tables IV and V.

vitro systems using a variety of markers ([^{3}H]sucrose by hepatocytes (27), ^{125}I-PVP and ^{198}Au by peritoneal macrophages (29), ^{198}Au and [^{14}C]sucrose by yolk sac (32), [^{3}H]inulin and [^{125}I]albumin in *Acanthamoeba* [5]). In most, if not all of these cases, the kinetics of release were biphasic, consisting of both a very fast component and a very slow component. For example, from the data of Pratten et al. (29), we calculated that rat peritoneal macrophages released previously accumulated ^{125}I-PVP with kinetics reflecting processes of 5- to 10-min and 800- to 900-min half-lives, whereas from the data of Ose et al. (27), we calculated that rat hepatocytes released previously accumulated ^{125}I-PVP with kinetics reflecting processes of 5- to 10-min and 300- to 400-min half-lives. In only one of these reports (27) was there an attempt to characterize this release to determine its significance. These workers found that release was greatly inhibited at 4°C, a finding consistent with our own. Considering the differences in cell types, experimental design, and methodology it seems more than fortuitous that these other systems also could be modeled in a manner similar to our scheme for alveolar macrophages and fibroblasts and yield such similar kinetic parameters. It remains to be seen if this is a feature common to all mammalian cells.

In contrast, there have been reports that the pinocytic markers, horseradish peroxidase (HRP) (38) and colloidal gold (8) do not get regurgitated into the culture medium. Concerning the report using HRP, the prolonged washing regimen used to remove the extracellular marker (30–60 min at 37°C) may explain why significant release was not observed in a subsequent 30-min reincubation. Concerning the report on colloidal gold, it is unclear why release was not observed in mouse peritoneal macrophages because release of colloidal gold was observed in rat peritoneal macrophages (29).

We believe that exocytosis of previously accumulated pinocytic marker ([^{14}C]sucrose) is a manifestation of a continuous, constitutive homeostatic process that may be set to a new steady state level, but is not turned on or off by an extracellular trigger. In this regard, we found that exocytosis was unaffected in both macrophages and fibroblasts by the removal of extracellular calcium and magnesium. This finding supports the above contention because it has been reported that in cells where secretion is also considered a continuous process (i.e. immunoglobulins by plasma cells [40], procollagen by fibroblasts [41], and secretory proteins by activated peritoneal macrophages [41]) exocytosis is independent of extracellular calcium, whereas in those cell types that secrete only when appropriately stimulated (classically, endocrine and exocrine gland cells, e.g. pancreatic beta cells [10], pancreatic acinar cells [18], adrenal medulla [13], and neurohypophysis [14]), exocytosis requires the presence of extracellular calcium.

There are alternative explanations for the results in this paper that need to be addressed. First, the kinetic compartments could result from a functionally heterogeneous cell population. We consider this possibility highly improbable because we have demonstrated that the two kinetic compartments are arranged sequentially. Second, Berlin et al. (2, 3) and Quintart et al. (31) have recently shown that endocytic function varies during the course of the cell cycle; notably, pinocytosis

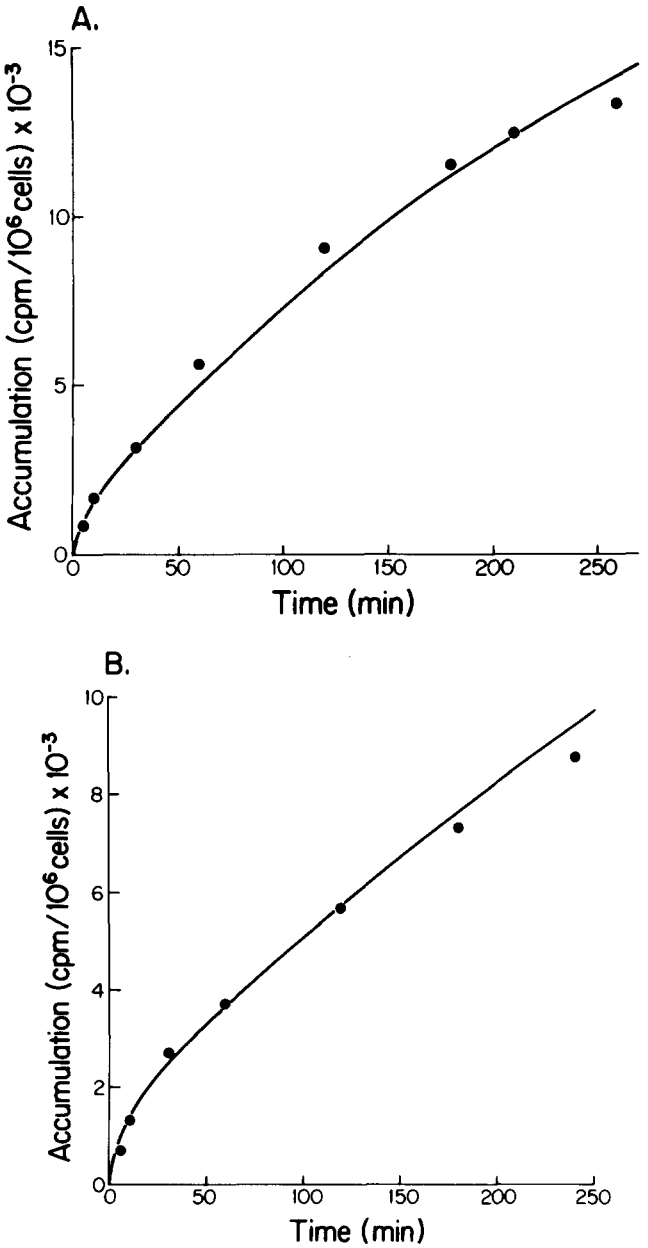

FIGURE 6 Comparison of computer-simulated time-courses for intracellular accumulation of [^{14}C]sucrose (solid line) with actual experimentally-determined values (●) for macrophages (*A*) and fibroblasts (*B*). Experimentally determined values of [^{14}C]sucrose accumulation by macrophages were those of Fig. 1 *A* and for fibroblasts those of Fig. 1 *B*. See text and Appendix II for details on computer-simulation.

is depressed during mitosis. Conceivably, this variable could confound interpretation of long-term kinetic studies in dividing cells, especially if the cells were synchronized. However, because normal pulmonary alveolar macrophages are an end-line cell (43), few, if any, of these cells undergo division in culture. Fibroblasts, on the other hand, are prolific in vitro, but because we have used confluent cultures of a nonsynchronized population, we believe that cell cycle associated changes in endocytic function are unlikely to have influenced our results in this cell type. Third, the possibility that permeation of intracellularly accumulated [^{14}C]sucrose contributes to release has not been entirely eliminated. However, we believe that this mechanism is unlikely to be a major consideration because (*a*) fluid-phase markers that possess charges and sizes distinctly different from [^{14}C]sucrose (e.g. ^{125}I-PVP) show release kinetics similar to that found for [^{14}C]sucrose (27, 29) and (*b*) amino acids modulate release kinetics in a manner not consistent with a diffusion-mediated mechanism (Besterman, Airhart and Low, manuscript submitted for publication).

The elegant work of Steinman, Brodie, and Cohn (37) was fundamental in establishing the dynamic nature of pinocytosis. Their morphological approach revealed that the HRP-reactive pinocytic vesicle space labeled completely within minutes after exposure to the enzyme, whereas the secondary lysosomal compartment required an hour to do so. Therefore, the most straightforward morphological correlate to our kinetically derived model of intracellular compartmentation is a scheme wherein pinosomes comprise our rapidly turning over compartment and (secondary) lysosomes comprise our slowly turning over compartment.

Assigning a distinct cellular substructure to each kinetically derived compartment provides a broader base for conjecture concerning the nature of the intercompartmental fluxes described, though the anatomical-to-kinetic correspondence is by no means proven. We have calculated that of the fluid entering the pulmonary alveolar macrophage per min, approximately two-thirds behave within an intracellular half-life of 5 min and one-third behaves with a half-life of 180 min (Table IV). This result can be interpreted in at least three ways. One scenario postulates that for a given pinosome, two-thirds of its contents rapidly egress from the cell while one-third continues on with the pinosome, fuses with the secondary lysosome, and pass through this slowly turning over compartment. The two other possibilities are both of the all-or-none type; that is, the entire contents of a single pinosome behaves identically. One of these latter models postulates that the pinosome population is homogenous, but the probability that a given pinosome rapidly fuses with the plasmalemma is twice that of that pinosome fusing with a secondary lysosome. The alternative hypothesis is that the pinosome population consists of two subpopulations, one of which rapidly recycles and one that fuses with the lysosome.

Table IV defined the sizes of compartments 1 and 2 and the intercompartmental fluxes in terms of the amount of radioactive sucrose that was associated with each compartment or flux at steady state. It is possible to calculate the corresponding volumes for these compartments and fluxes assuming that the cell cannot concentrate sucrose. By dividing the sizes and fluxes given in Table IV by the concentration of [^{14}C]sucrose radioactivity in the original media (27 cpm/nl for macrophages; 39 cpm/nl for fibroblasts), the volumes and fluxes listed in Table V were obtained. These compartmental volumes and fluxes were next expressed as a percent of total cell volume. When the relative compartmental volumes for alveolar macrophages are compared to the relative volumes of the pinosomal and secondary lysosomal compartments in peritoneal macrophages as determined by stereology by Steinman et al. ([37]; 2.65 and 2.53% of total cell volume, respectively), we find that the relative volume calculated for compartment 1 (2.1–2.7% of total cell volume) is in excellent agreement with their determination for pinosomes (2.65% of total cell volume) whereas the relative volume calculated for compartment 2 (37–49% of total cell volume) is 15–20 times greater than their determination for secondary lysosomes (2.53% of total cell volume). This apparent discrepancy warrants further attention. From the literature, it is clear that the volume of the vacuolar system is extremely sensitive to environmental conditions (8). The peritoneal macrophages on which Steinman et al. made measurements were cultured under conditions known to favor a small lysosomal space (37) whereas our culture conditions for alveolar macrophages are likely to have maximized the lysosomal space (21). Therefore, it is probable that conditions were optimal for detecting a difference. Even with this consideration in mind, the magnitude of the discrepancy makes it hard to avoid concluding that either (*a*) pinocytosed [^{14}C]sucrose redistributed to cellular compartments other than lysosomes or (*b*) that our calculated volume is spurious because the [^{14}C]sucrose has become concentrated inside the lysosomes. The first interpretation is tempting because of its simplicity and an interconnecting network such as GERL (26) could conceivably provide access to other cellular compartments. However, we are unaware of any data demonstrating distribution of fluid-phase

TABLE V

Apparent Volume Relationships Among Intracellular Compartments Involved in Fluid-Phase Pinocytosis

	Macrophages		Fibroblasts	
	Compartment 1	Compartment 2	Compartment 1	Compartment 2
Apparent volume (nl/10^6 cells)	41	740	42	769
Percent of total cell volume*	2.1–2.7	37–49	1.7	26–31
K_{efflux} (nl/min·10^6 cells)	5.7	2.9	3.6–4.8	0.85–1.23
K_{efflux} (percent of total cell volume/min)*	0.29–0.38	0.15–0.19	0.12–0.20	0.03–0.05
Total K_{efflux} = Total K_{influx} (nl/min·10^6 cells)	8.6		4.5–6.0	
Total K_{influx} (percent of total cell volume/min)*	0.44–0.57		0.15–0.25	
Total K_{influx} (percent of total cell volume/h)*	26–34		9.0–15	

Values were determined by analyzing the data in Table IV as described in text.

* The total cell volume for guinea pig alveolar macrophages was taken to be equivalent to 1.5–2.0 μl/10^6 cells as determined by J. Porter, J. A. Airhart, and R. B. Low (unpublished observations). The total cell volume for confluent IMR-90 fibroblasts (population doubling level 20–30) was taken to be 2.5–3.0 μl/10^6 cells as determined by Houghton and Stidworthy (19).

markers to compartments others than secondary lysosomes. Therefore, if we are to conclude that a fluid-phase marker (i.e. [^{14}C]sucrose) can be concentrated inside a compartment of the cell (e.g. the lysosome), this poses theoretical and practical implications for interpretation of a kinetic analysis of cellular dynamics.

First, we will consider the impact on the applicability of and values for the kinetic constants and the volumes of the two intracellular compartments. Because our determination of the volume of compartment 1 closely matched the volume of its most likely anatomical identity, namely the pinosomal compartment, it is reasonable to assume that the magnitudes of our calculated kinetic constants K_1, K_2, K_3, and k_3 and the calculated volume of compartment 1 characterize the behavior of both [^{14}C]sucrose and its associated fluid volume equally well. However, in light of the possibility that [^{14}C]sucrose can be concentrated in compartment 2 (e.g. the lysosome), the flux of the accompanying water must be even faster. Therefore, the magnitude of the calculated kinetic constants, k_2 and k_4 and the size of compartment 2 pertain to [^{14}C]sucrose only, whereas K_4 must apply to both [^{14}C]sucrose and water because K_4 must equal K_2. Based on these considerations we can find no reason to believe that the possibility of intracellular concentration of the fluid-phase marker, [^{14}C]sucrose, in any way obviates our conclusions that the cell behaves kinetically as if it consists of at least a 2 compartment system arranged in series, one compartment turning over very rapidly and the other relatively slowly.

Although there is some suggestion in the literature that concentration of solutes may occur during the intracellular processing of pinosomes, the mechanisms underlying this phenomenon are not clear at this time. Steinman et al. (37) felt that it was unlikely that internalized vesicle fluid was returned to the extracellular space by vesicular packaging. Instead, they postulated that internalized fluid is lost by shifts across the newly forming secondary lysosomal membrane during pinosome-lysosome fusion, though they were unable to predict how such a mechanism might operate. However, this concept of intracellular fluid shifts provides a possible mechanism for concentrating solute and is soundly rooted in the observations that the secondary lysosome membrane is semipermeable, causing the vacuolar space to behave as an osmometer (9). In addition, it is thought that incoming pinosomes shrink during their intracellular travels, though whether this shrinkage occurs before, during, or after fusion with the secondary lysosome is controversial (15, 37).

Studies on the fate of nondegradable pinocytic substrates have emphasized their retention within full and effete lysosomes or so-called residual bodies (11). These residual bodies are thought to provide a terminal sink for pinocytic substrates, functionally acting as a third compartment in addition to pinosomes and active secondary lysosomes. Therefore, with respect to our model in Fig. 5, we have considered the possibility of a third compartment (compartment 3) in series with compartments 1 and 2 and have designed this third compartment to act as a dead-end repository (Fig. 7). We then asked at what rate could compartment 3 fill (with fractional rate constant k_5) from compartment 2 and yet show accumulation kinetics essentially indistinguishable from those observed. By computer-simulation (Appendix II B) we found that k_5 could be as great as 0.08%/min (20% of k_4) before overall predicted and observed kinetics became incongruent within the first 4 h (Fig. 8). This is an important finding because it accomodates

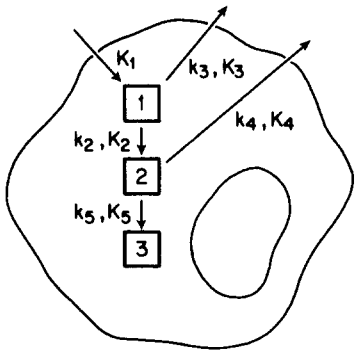

FIGURE 7 Modified model depicting the kinetically defined compartments and fluxes involved in fluid-phase pinocytosis and exocytosis in alveolar macrophages and fibroblasts. *K*'s are absolute rate constant's and *k*'s fractional rate constants. Their values are given in text and Tables IV and V.

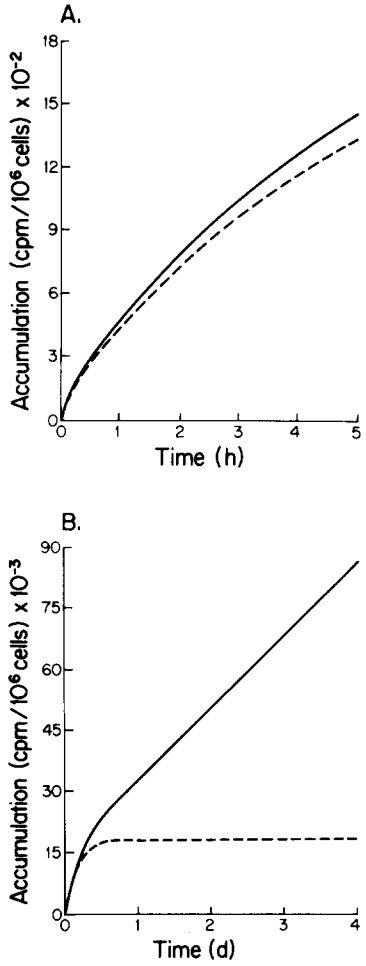

FIGURE 8 Comparison of computer predicted kinetics of accumulation of [^{14}C]sucrose by macrophages for 2 compartment (- - -) and 3 compartment models (——). The two models are compared over a period of hours (*A*) or days (*B*). The kinetic parameters used to stimulate the time-course of accumulation are given in Appendix IIA for 2 compartment model and Appendix IIB for 3 compartment model.

both nonlinear accumulation on a scale of hours but nearly linear accumulation on a scale of days – a prediction consonant with the findings of others (45). Because compartment 3 must fill with such a long half-life, we cannot detect its presence

within our experimental time course (Fig. 8). Further investigation of long term kinetics will be necessary, therefore, to determine whether the 2 or 3 compartment model best describes results from our experimental systems.

Quantitation of pinocytosis, both fluid-phase and absorptive, has been performed previously using a variety of markers and numerous in vitro systems (3, 4, 5, 21, 27, 29, 31, 32, 33, 38, 39, 43). To equate accumulated intracellular marker with an absolute endocytic rate in all these studies, it was assumed that the marker, once internalized, could not exit from the cell. However, in light of our results as supported by those mentioned above, the validity of this assumption must be questioned seriously. If this assumption was not correct then all pinocytic rates measured beyond the first few minutes of incubation would be underestimates of the true pinocytic rate. This notion is bolstered by the findings of Steinman et al. (37): stereological measurements made after 0–5 min of exposure to HRP at 37° showed that peritoneal macrophages internalized extracellular fluid at a rate equivalent to 26% of their cell volume per hour, or the equivalent of 102 nl/h per 10^6 macrophages while L-cells in log phase growth internalized at a rate equivalent to 3% of their cell volume per hour or the equivalent of 54 nl/h per 10^6 fibroblasts. However, when these workers quantitated accumulation by enzymatic assay after longer exposures to HRP, their calculated rates decreased to only 72 nl/h per 10^6 peritoneal macrophages and 32 nl/h per 10^6 fibroblasts. As can be seen from Table V, our calculated initial rates translate into turnover of cellular volume on the order of 26–34%/h in alveolar macrophages and 9–15%/h in confluent lung fibroblasts, findings consistent with those for peritoneal macrophages (see above, [37]) and for confluent L-cells, respectively (confluent L-cells pinocytose at a rate 2–4 times greater than L-cells in log phase growth; see above, [39]).

However, in neither cell type described in this paper were we able to measure directly the actual initial rate of [^{14}C]sucrose uptake. The linear accumulation obtained over the first 10 min are only apparent, resulting from the serendipitous sum of two compartments in series. The slope over the first 10 min underestimates the calculated initial rate by 30% in macrophages and 23–43% in fibroblasts. These results emphasize that the bulk of intracellular turnover of engulfed solute and solvent is very rapid. This condition requires that the initial rate of pinocytosis be determined at very early times. Unfortunately, it technically becomes very difficult to quantitate the intracellular accumulation of an extracellular marker over time intervals shorter than 5 min because the volume engulfed during a very short interval approaches the residual volume of extracellular medium that cannot be easily washed from the cell layer and thus constitutes an unreducible level of background noise.

Fortunately, alternatives to the method we have discussed above exist. One of these is to monitor the kinetics of exocytosis and then to use these data to calculate the rate of endocytosis as we have done in this paper. We have shown that, at least for fibroblasts and macrophages, accurate information concerning the movement of water into the cell (K_1) can be obtained by quantitating efflux of [^{14}C]sucrose from compartment 1 (K_3) and adding to it efflux from compartment 2 (K_4); i.e. $K_1 = K_3 + K_4$. Another alternative is to quantitate the initial pinocytic rate by monitoring the appearance of labeled pinocytic vesicles over very short intervals by electron microscopy (37–39). This approach is not subject to the same limitations as chemical or radioisotopic analysis, but possesses its own set of restrictions.

The difficulty in correctly assessing pinocytic function is of concern not only to those interested in the absolute rate of pinocytosis, but also under conditions where only relative rates are required. Failure to determine the true magnitude of early events in pinocytosis may introduce significant errors of interpretation, especially in cases involving changes in flux without concomitant changes in compartmental volumes.

In summary, our results provide the first direct experimental evidence that the majority of fluid-phase marker internalized in pinocytic vesicles is rapidly exocytosed from the cell. That such must be the case was predicted by Steinman et al. (37) based on morphological and theoretical considerations. Our demonstration of the dynamic nature of cellular fluid balance, together with the published observations of rapid membrane recycling (25, 34), strongly support the concept that endo- and exocytosis are coupled, multicompartmental processes that provide an overall mechanism for cellular volume homeostasis.

APPENDIX I

This approach to compartmental analysis was derived by R. C. Woodworth while participating in a course taught by the late Dr. Dan F. Bradley.

Consider the system:

$$X \xrightarrow[K_1]{k_1} R \xrightarrow[K_2]{k_2} S \xrightarrow[K_3]{k_3} U \xrightarrow[K_4]{k_4} \ldots Z$$

where

k_i = fractional rate constant with units time $^{-1}$

K_i = absolute rate constant with units activity · time $^{-1}$

Assume the following about the system:

1. Reaction time is limited to initial appearance of activity (changes in specific activity (α) depends only on input).
2. The system is in steady state:

$$\frac{d[R]}{dt} = \frac{d[S]}{dt} = \frac{d[U]}{dt} = 0$$

3. At t = 0, tracer is introduced into compartment X.

$$\frac{d[R]\alpha_R}{dt} = k_1[X]\alpha_X = K_1.$$

$$\alpha_R = \frac{K_1 t}{[R]}.$$

$$\frac{d[S]\alpha_S}{dt} = k_2[R]\alpha_R = k_2[R]\frac{K_1 t}{[R]} = k_2 K_1 t.$$

$$\alpha_S = \frac{K_1 k_2 t^2}{2[S]}.$$

$$\frac{d[U]\alpha_U}{dt} = k_3[S]\alpha_S = \frac{k_3[S]K_1 k_2 t^2}{2[S]} = \frac{K_1 k_2 k_3 t^2}{2}.$$

$$[U]\alpha_U = \frac{K_1 k_2 k_3 \cdot t^3}{6}.$$

Therefore, a plot of the product $[Z]\alpha_Z$, which is equivalent to the activity in Compartment Z, vs. t^n will give a straight line passing through the origin only when the value chosen for n correctly indicates which intermediate Z is from X. The slope of this line equals $\frac{K_1 k_2 k_3 \ldots k_n}{n!}$

APPENDIX II

For computer simulation of intracellular accumulation of [^{14}C]sucrose the equations listed below were used to describe the flux of isotope into and out of each intracellular compartment at steady state. The program was written in FORTRAN-IV and performed on a DEC System 2060.

Two Compartment Model

$$\text{cpm } 1_T = \text{cpm } 1_{T-1} + K_1 \Delta t - k_2 \Delta t \text{ cpm } 1_{T-1} - k_3 \Delta t \text{ cpm } 1_{T-1}.$$

$$\text{cpm } 2_T = \text{cpm } 2_{T-1} + k_2 \Delta t \text{ cpm } 1_{T-1} - k_4 \Delta t \text{ cpm } 2_{T-1}.$$

where:

cpm i_T (i = 1, 2, or 3) = cpm in compartment i at the end of time-step T ($T \geq 1$; i.e. for the first computation, $T = 1$).

initial value of cpm $i_{T-1} = 0$ when $T = 1$.

Δt = length of time-step (e.g. 0.025 min.).

K_1, k_2, k_3, k_4, were constants whose values were given as follows:

Macrophages: $K_1 = 234$ cpm/min · 10^6 cells; $k_2 = 7\%$/min; $k_3 = 14\%$/min; $k_4 = 0.4\%$/min.

Fibroblasts: $K_1 = 200$ cpm/min · 10^6 cells; $k_2 = 2.4\%$/min; $k_3 = 10\%$/min; $k_4 = 0.13\%$/min.

Values were computed for 10^4 time-steps.

Three Compartment Model

$$\text{cpm } 1_T = \text{cpm } 1_{T-1} + K_1 \Delta t - k_2 \Delta t \text{ cpm } 1_{T-1} - k_3 \Delta t \text{ cpm } 1_{T-1}.$$

$$\text{cpm } 2_T = \text{cpm } 2_{T-1} + k_2 \Delta t \text{ cpm } 1_{T-1} - k_4 \Delta t \text{ cpm } 2_{T-1} - k_5 \Delta t \text{ cpm } 2_{T-1}.$$

$$\text{cpm } 3_T = \text{cpm } 3_{T-1} + k_5 \Delta t \text{ cpm } 2_{T-1}.$$

K_1, k_2, k_3, k_4, and k_5 were given as follows:

Macrophages: $k_1 = 249$ cpm/min · 10^6 cells; $k_2 = 7\%$/min; $k_3 = 14\%$/min; $k_4 = 0.4\%$/min; $k_5 = 0.08\%$/min.

Values were computed for 10^4 time-steps.

The authors wish to thank Dr. Marlene Absher for providing the fibroblasts, Joanne Bordeaux and Janet Arnold for expert technical assistance, Jackie Fischl for writing the computer program, Dr. C. C. Widnell for suggesting the control experiment involving invertase, and Polly Ann Brenker for typing the manuscript.

This research was supported by National Heart, Lung, and Blood Institute (NHLBI) Grant No. HL-14212 (Pulmonary SCOR) and NHLBI Training Grant No. T32-HL07206 sponsored by the Vermont Lung Center.

Received for publication 21 April 1981, and in revised form 21 July 1981.

REFERENCES

1. Becker, G., and M. J. Ashwood-Smith. 1973. Endocytosis by Chinese hamster fibroblasts. *Exp. Cell Res.* 82:310–314.
2. Berlin, R. D., J. M. Oliver, and R. J. Walter. 1978. Surface functions during mitosis. I. Phagocytosis, pinocytosis and mobility of surface-bound Con A. *Cell.* 15:327–341.
3. Berlin, R. D., and J. M. Oliver. 1980. Surface functions during mitosis II. Quantitation of pinocytosis and kinetic characterization of the mitotic cycle with a new fluorescence technique. *J. Cell Biol.* 85:660–671.
4. Besterman, J. M., J. A. Airhart, and R. B. Low. 1982. Macrophage phagocytosis: analysis of particle binding and internalization. *Am. J. Physiol.* In press.
5. Bowers, B., and T. E. Olszewki. 1972. Pinocytosis in *Acanthamoeba castellanii. J. Cell Biol.* 53:681–694.
6. Bowers, B., T. E. Olszewski, and J. Hyde. 1981. Morphometric analysis of volumes and surface areas in membrane compartments during endocytosis in *Acanthamoeba. J. Cell Biol.* 88:509–515.
7. Brewer, D. B., and D. Heath. 1963. Lysosomes and vacuolation of the liver cell. *Nature (Lond.).* 198:1015–1016.
8. Cohn, S. A., and B. Benson. 1965. The in vitro differentiation of monolayer phagocytes. III. The reversibility of granule and hydrolytic enzyme formation and the turnover of granule constituents. *J. Exp. Med.* 122:455–466.
9. Cohn, Z. A., and B. A. Ehrenreich. 1969. The uptake, storage and intracellular hydrolysis of carbohydrates by macrophages. *J. Exp. Med.* 129:201–225.
10. Curry, D. L., L. L. Bennett, and G. W. Grodsky. 1968. Dynamics of insulin secretion by the perfused rat pancreas. *Endocrinology.* 83:572–584.
11. Daems, W. Th., E. Wisse, and P. Brederoo. 1972. *In:* Lysosomes: A Laboratory Handbook. J. T. Dingle, editor. North-Holland Publishing Co., Amsterdam. 183–189.
12. Davies, P. F., and R. Ross. 1978. Mediation of pinocytosis in cultured arterial smooth muscle and endothelial cells by platelet-derived growth factor. *J. Cell Biol.* 79:663–671.
13. Douglas, W. W. 1966. The mechanism of release of catecholamines from adrenal medulla. *Pharmacol. Rev.* 18:471–480.
14. Douglas, W. W., and A. M. Poisner. 1964. Stimulus-secretion coupling in a neurosecretory organ: the role of calcium in the release of vasopressin from the neurohypophysis. *J. Physiol.* 172:1–18.
15. Duncan, R., and M. K. Pratten. 1977. Membrane economics in endocytic systems. *J. Theor. Biol.* 66:727–735.
16. Fell, H. B., and J. T. Dingle. 1969. Endocytosis of sugars in embryonic skeletal tissues in organ culture. I. *J. Cell Sci.* 4:89–103.
17. Frost, A. A., and R. G. Pearson. 1961. Kinetics and Mechanism. Wiley, New York, second edition.
18. Hokin, L. E. 1966. Effects of calcium omission on acetylcholine-stimulated amylase secretion and phospholipid synthesis in pigeon pancreas slices. *Biochim. Biophys. Acta.* 115:219–221.
19. Houghton, B. A., and G. H. Stidworthy. 1979. A growth history comparison of the human diploid cells WI-38 and IMR-90: proliferative capacity and cell sizing analysis. *In Vitro (Rockville)* 15:697–702.
20. Jacques, P. 1969. Lysosomes in Biology and Pathology. J. T. Dingle and H. B. Fell, editors. North-Holland Press, Amsterdam. 2:395.
21. Kaplan, J., and M. Nielsen. 1978. Pinocytic activity of rabbit alveolar macrophages *in vitro. J. Reticuloendothel. Soc.* 24:673–685.
22. Lee, G. T. Y., and D. L. Engelhardt. 1977. Protein metabolism during growth of Vero cells. *J. Cell. Physiol.* 92:293–302.
23. Low, R. B. 1974. Protein biosynthesis by the pulmonary alveolar macrophages: conditions of assay and the effects of cigarette smoke extracts. *Am. Rev. Respir. Dis.* 110:466–477.
24. Lowry, O., N. Rosebrough, A. Farr, and R. Randall. 1951. Protein measurements with the Folin phenol reagent. *J. Biol. Chem.* 193:265–275.
25. Muller, W. A., R. M. Steinman, and Z. A. Cohn. 1980. The membrane proteins of the vacuolar system II. Directional flow between secondary lysosomes and plasma membrane *J. Cell Biol.* 86:304–314.
26. Novikoff, A. B. 1976. The endoplasmic reticulum: a cytochemist's view (A review). *Proc Natl. Acad. Sci. U. S. A.* 73:2781–2787.
27. Ose, L., T. Ose, R. Reinertsen, and T. Berg. 1980. Fluid endocytosis in isolated rat parenchymal and non-parenchymal liver cells. *Exp. Cell Res.* 126:109–119.
28. Phaire-Washington, L., F. Wang, and S. C. Silverstein. 1980. Phorbol myristate acetate stimulates pinocytosis and membrane spreading in mouse peritoneal macrophages. *J. Cell Biol.* 86:634–640.
29. Pratten, M. K., K. E. Williams, and J. B. Lloyd. 1977. A quantitative study of pinocytosis and intracellular proteolysis in rat peritoneal macrophages. *Biochem. J.* 168:365–372.
30. Putman, E. W. 1957. Paper chromatography of sugars. *In:* Methods of Enzymology. S. P. Colowick and N. O. Kaplan, editors. Academic Press, Inc., New York 3 and 62–72.
31. Quintart, J., M. A. Leroy-Houyet, A. Trouet, and P. Baudhuin. 1979. Endocytosis and chloroquine accumulation during the cell cycle of hepatoma cells in culture. *J. Cell Biol.* 82:644–653.
32. Roberts, A. V. S., K. E. Williams, and J. B. Lloyd. 1977. the pinocytosis of ^{125}I-labeled poly (vinylpyrrolidone), ^{14}C-sucrose and colloidal ^{198}Augold by rat yolk sac cultured *in vitro. Biochem. J.* 168:239–244.
33. Schneider, Y. J., P. Tulkens, C. deDuve, and A. Trouet. 1979. Fate of plasma membrane during endocytosis I. Uptake and processing of anti-plasma membrane and control immunoglobulins by cultured fibroblasts. *J. Cell Biol.* 82:449–465.
34. Schneider, Y. J., P. Tulkens, C. Duve, and A. Trouet. 1979. Fate of plasma membrane during endocytosis. II. Evidence for recycling (shuttling) of plasma membrane constituents. *J. Cell Biol.* 82:466–474.
35. Segal, I. H. 1976. In Biochemical Calculations. 2nd edition. Wiley, New York 228.
36. Sillen, L. B., and A. E. Martell. 1971. *In:* Stability Constants of Metal-Ion Complexes. Supplement No. 1., Special Publication No. 25. The Chemical Society. Burlington House, London. 624 and 626.
37. Steinman, R. M., S. E. Brodie, and Z. A. Cohn. 1976. Membrane flow during pinocytosis. *J. Cell Biol.* 68:665–687.
38. Steinman, R. M., and Z. A. Cohn. 1972. The interaction of soluble horseradish peroxidase with mouse peritoneal macrophages in vitro. *J. Cell Biol.* 55:186–204.
39. Steinman, R. M., J. M. Silver, and Z. A. Cohn. 1974. Pinocytosis in fibroblasts. *J. Cell Biol.* 63:949–969.
40. Tartakoff, A. M., and P. Vassalli. 1977. Plasma cell immunoglobulin secretion. *J. Exp. Med.* 146:1332–1345.
41. Tartakoff, A. M., and P. Vassalli. 1978. Comparative studies of intracellular transport of secretory proteins. *J. Cell Biol.* 79:694–707.
42. Thilo, L., and G. Vogel. 1980. Kinetics of membrane internalization and recycling during pinocytosis in *Dictyostelium discoideum. Proc. Natl. Acad. Sci. U. S. A.* 77:1015–1019.
43. Van Furth, R. 1970. Origin and kinetics of monocytes and macrophages. *Semin. Hematol.* 7:125–141.
44. Wagner, R., M. Rosenberg, and R. Estensen. 1971. Endocytosis in Chang liver cells. *J. Cell Biol.* 50:804–817.
45. Williams, K. E., E. M. Kidston, F. Beck, and J. B. Lloyd. 1975. Quantitative studies of pinocytosis. I. Kinetics of uptake of [^{125}I]polyvinylpyrrolidine by rat yolk sac cultured in vitro. *J. Cell Biol.* 64:113–122.